

# K<sub>IR</sub> channels function as electrical amplifiers in rat vascular smooth muscle

Pamela D. Smith<sup>1</sup>, Suzanne E. Brett<sup>1</sup>, Kevin D. Luykenaar<sup>1</sup>, Shaun L. Sandow<sup>2</sup>, Sean P. Marrelli<sup>3</sup>, Edward J. Vigmond<sup>4</sup> and Donald G. Welsh<sup>1</sup>

<sup>1</sup>Smooth Muscle Research Group and Department of Physiology & Biophysics, University of Calgary, Calgary, Alberta, Canada

<sup>2</sup>Department of Pharmacology, University of New South Wales, Sydney, Australia

<sup>3</sup>Department of Anesthesiology, Department of Molecular Physiology & Biophysics and Department of Cardiovascular Sciences, Baylor College of Medicine, Houston, TX, USA

<sup>4</sup>Department of Electrical and Computer Engineering, University of Calgary, Alberta, Canada

Strong inward rectifying K<sup>+</sup> (K<sub>IR</sub>) channels have been observed in vascular smooth muscle and can display negative slope conductance. In principle, this biophysical characteristic could enable K<sub>IR</sub> channels to ‘amplify’ responses initiated by other K<sup>+</sup> conductances. To test this, we have characterized the diversity of smooth muscle K<sub>IR</sub> properties in resistance arteries, confirmed the presence of negative slope conductance and then determined whether K<sub>IR</sub> inhibition alters the responsiveness of middle cerebral, coronary septal and third-order mesenteric arteries to K<sup>+</sup> channel activators. Our initial characterization revealed that smooth muscle K<sub>IR</sub> channels were highly expressed in cerebral and coronary, but not mesenteric arteries. These channels comprised K<sub>IR</sub>2.1 and 2.2 subunits and electrophysiological recordings demonstrated that they display negative slope conductance. Computational modelling predicted that a K<sub>IR</sub>-like current could amplify the hyperpolarization and dilatation initiated by a vascular K<sup>+</sup> conductance. This prediction was consistent with experimental observations which showed that 30 μM Ba<sup>2+</sup> attenuated the ability of K<sup>+</sup> channel activators to dilate cerebral and coronary arteries. This attenuation was absent in mesenteric arteries where smooth muscle K<sub>IR</sub> channels were poorly expressed. In summary, smooth muscle K<sub>IR</sub> expression varies among resistance arteries and when channel are expressed, their negative slope conductance amplifies responses initiated by smooth muscle and endothelial K<sup>+</sup> conductances. These findings highlight the fact that the subtle biophysical properties of K<sub>IR</sub> have a substantive, albeit indirect, role in enabling agonists to alter the electrical state of a multilayered artery.

(Received 23 September 2007; accepted after revision 3 December 2007; first published online 6 December 2007)

**Corresponding author** D. G. Welsh: Smooth Muscle Research Group, HMRB-G86, Heritage Medical Research Building, University of Calgary, 3330 Hospital Dr NW, Calgary, Alberta, Canada, T2N 4N1. Email: dwelsh@ucalgary.ca

The magnitude and distribution of tissue blood flow is controlled by an integrated network of resistance arteries (Segal & Duling, 1986; Segal, 2000). Under dynamic conditions, tone within an arterial network is regulated by multiple stimuli initiated by changes in intraluminal pressure (Bayliss, 1902; Knot & Nelson, 1998), blood flow (Garcia-Roldan & Bevan, 1990; Koller & Kaley, 1991), neuronal activity (Brayden & Bevan, 1985; Si & Lee, 2002) and tissue metabolism (Harder *et al.* 1998; Filosa *et al.* 2006). Vasoactive stimuli influence arterial diameter by activating signal transduction pathways which control myofilament Ca<sup>2+</sup> sensitivity (Somlyo & Somlyo, 2003) and/or cytosolic [Ca<sup>2+</sup>] (Nelson *et al.* 1990; Nelson & Quayle, 1995). Cytosolic [Ca<sup>2+</sup>] is, in turn, tightly coupled to membrane potential (V<sub>M</sub>) and the graded influx of Ca<sup>2+</sup>

through voltage-operated Ca<sup>2+</sup> channels (Nelson *et al.* 1990; Nelson & Quayle, 1995).

To initiate changes in smooth muscle V<sub>M</sub>, vasoactive agents must directly regulate an ionic conductance. This regulation is frequently viewed in simple terms with stimuli activating transduction pathways that control kinases and phosphatases responsible for channel phosphorylation (Nelson *et al.* 1990; Nelson & Quayle, 1995). Although direct regulation is essential, this is often interpreted to suggest that only these currents alter the electrical and mechanical state of vascular smooth muscle. This view overlooks the potential contribution of ionic conductances whose voltage-dependent properties could in essence ‘facilitate’ or ‘amplify’ an electrical response initiated by another agonist-sensitive channel.

Of particular interest is the strong inward rectifying  $K^+$  ( $K_{IR}$ ) current which over the physiological voltage range displays negative slope conductance. (Matsuda *et al.* 2003; Schram *et al.* 2003; Dhamoon *et al.* 2004). Briefly, negative slope conductance refers to an inherent ability of some  $K_{IR}$  channels to increase their activity as a cell hyperpolarizes (Nelson *et al.* 1990; Nelson & Quayle, 1995). Such an increase contrasts with the situation for other vascular  $K^+$  channels and is dependent upon the relief of a voltage-dependent  $Mg^{2+}$ /polyamine block (Nelson & Quayle, 1995; Robertson *et al.* 1996; Matsuda *et al.* 2003). Negative slope conductance is typically observed in channels composed of  $K_{IR}2.1$  and 2.2 subunits and these constituents are often expressed in vascular smooth muscle (Bradley *et al.* 1999; Karkanis *et al.* 2003; Wu *et al.* 2007). While smooth muscle  $K_{IR}$  channels could, theoretically, amplify arterial responses, the supporting experimental evidence remains limited.

To explore whether smooth muscle  $K_{IR}$  channels operate as electrical amplifiers, we characterized  $K_{IR}$  expression in resistance arteries, confirmed negative slope conductance and then determined whether channel inhibition influenced the responsiveness of middle cerebral, coronary septal and third-order mesenteric arteries to  $K^+$  channel activators. Findings show that smooth muscle  $K_{IR}$  channels are differentially expressed among resistance arteries, and when present are composed of  $K_{IR}2.1$  and 2.2 subunits displaying negative slope conductance. Computational and experimental analyses reveal that this biophysical property enables smooth muscle  $K_{IR}$  to augment the electrical and vasomotor responses initiated by other smooth muscle or endothelial  $K^+$  channels. These findings demonstrate that subtle channel properties are important for the regulation of arterial responsiveness. They also indicate that an ionic conductance need not be directly regulated by an agonist to significantly alter the electrical and mechanical state of vascular smooth muscle.

## Methods

### Animal procedures

Animal procedures were approved by the Animal Care and Use Committee at the University of Calgary. Briefly, female Sprague–Dawley rats (10–12 weeks of age) were killed via carbon dioxide asphyxiation. The brain, heart and mesentery were carefully removed and placed in cold phosphate-buffered (pH 7.4) saline solution containing (mM): NaCl 138, KCl 3,  $Na_2HPO_4$  10,  $NaH_2PO_4$  2, glucose 5,  $CaCl_2$  0.1 and  $MgSO_4$  0.1. Middle cerebral, coronary septal and third-order mesenteric arteries were carefully dissected out of surrounding tissue and cut into 2 mm segments.

### Vessel myography

Arterial segments were mounted in a customized arteriograph and superfused with warm (37°C) physiological salt solution (PSS; pH 7.4) containing (mM): NaCl 119, KCl 4.7,  $NaHCO_3$  20,  $KH_2PO_4$  1.1,  $MgSO_4$  1.2,  $CaCl_2$  1.6 and glucose 10. With the exception of vessels used for experiments in Fig. 9, endothelial cells were removed from all vessels by passing air bubbles through the vessel lumen (2–4 min); successful removal was confirmed by the loss of acetylcholine- or bradykinin-induced dilatation. Arteries were equilibrated for 60 min and contractile responsiveness assessed by brief (~10 s) exposure of the tissue to 60 mM KCl. Following equilibration, arteries were maintained in a hyperpolarized (15 mmHg intravascular pressure) or depolarized (80 mmHg + 0.01–1  $\mu$ M phenylephrine) state. Vessels were then exposed to one of four experimental protocols: (1)  $Ba^{2+}$  (30  $\mu$ M) alone; (2) elevated extracellular  $[K^+]$  (raised from 5.8 or 4.0 to 15.0 mM)  $\pm$   $Ba^{2+}$  or ouabain (100 nM); (3) P-1075 or pinacidil (0.01–10  $\mu$ M,  $K_{ATP}$  channel openers)  $\pm$   $Ba^{2+}$ ; or (4) superfused acetylcholine (0.1–10  $\mu$ M) or intraluminal uridine triphosphate (UTP, 2  $\mu$ M)  $\pm$   $Ba^{2+}$ . Control experiments confirmed that glybenclamide (10  $\mu$ M) blocked the ability of cerebral ( $n = 2$ ) and coronary ( $n = 2$ ) arteries to dilate in response to P-1075 (1  $\mu$ M) and pinacidil (1  $\mu$ M), respectively. Arterial diameter was monitored using an automated edge detection system (IonOptix, Milton, MA, USA). Smooth muscle  $V_M$  was assessed by inserting a glass microelectrode backfilled with 1 M KCl (tip resistance, 120–150 M $\Omega$ ) into the vessel wall. The criteria for successful cell impalement included: (1) a sharp negative  $V_M$  deflection upon entry; (2) a stable recording for at least 1 min following entry; and (3) a sharp return to baseline upon electrode removal.

### Isolation of arterial smooth muscle cells

Smooth muscle cells from middle cerebral, coronary septal and third-order mesenteric arteries were enzymatically isolated as previously described (Welsh & Brayden, 2001; Luykenaar *et al.* 2004). Briefly, arterial segments were placed in an isolation medium (37°C, 10 min) containing (mM): NaCl 60, sodium glutamate 80, KCl 5,  $MgCl_2$  2, glucose 10 and Hepes 10 with 1 mg ml<sup>-1</sup> albumin (pH 7.4). Vessels were then exposed to a two-step digestion process that involved: (1) a 10–20 min incubation in isolation media (37°C) containing 0.6 mg ml<sup>-1</sup> papain and 1.8 mg ml<sup>-1</sup> dithioerythritol; and (2) a 10–20 min incubation in isolation medium containing 100  $\mu$ M  $Ca^{2+}$ , 0.7 mg ml<sup>-1</sup> type F collagenase and 0.4 mg ml<sup>-1</sup> type H collagenase. Following treatment, tissues were washed repeatedly with ice-cold isolation medium and triturated

with a fire-polished pipette. Liberated cells were stored in ice-cold isolation medium for use the same day.

### Electrophysiology

Conventional patch-clamp electrophysiology was used to measure whole-cell currents in isolated smooth muscle cells. Briefly, recording electrodes (resistance, 4–7 M $\Omega$ ) were fashioned from borosilicate glass, covered in sticky wax to reduce capacitance, and backfilled with solution containing (mM): NaCl 5, KCl 35, potassium gluconate 100, CaCl<sub>2</sub> 1, Hepes 10, EGTA 10, Tris-ATP 2.5 and GTP 0.2 (pH 7.2). This pipette was then gently lowered onto a cell and negative pressure applied to rupture the membrane. Cells with an input resistance greater than 10 G $\Omega$  were then voltage clamped (–60 mV) and equilibrated for 15 min in a bath solution containing (mM): NaCl 135, KCl 5, MgCl<sub>2</sub> 0.1, Hepes 10, glucose 5 and CaCl<sub>2</sub> 0.1 (pH 7.4). Following equilibration, bath [K<sup>+</sup>] was elevated from 5 to 60 mM via equimolar replacement of NaCl by KCl. K<sub>IR</sub> activity was then assessed by ramping cells between –120 and 20 mV (0.047 mV ms<sup>–1</sup>), and quantifying the component of the whole-cell current that was sensitive to 30  $\mu$ M Ba<sup>2+</sup>. Control experiments monitoring the glybenclamide-sensitive (10  $\mu$ M; at –80 mV with 60 mM extracellular K<sup>+</sup>) and the iberiotoxin-sensitive (100 nM; +20 mV) currents confirmed that the pipette solution minimized K<sub>ATP</sub>-activated and Ca<sup>2+</sup>-activated K<sup>+</sup> (K<sub>Ca</sub>) channel activity, respectively. Whole-cell currents were recorded on an Axopatch 200B amplifier (Axon Instruments, Union City, CA, USA), filtered at 1 kHz, digitized at 5 kHz and stored on a computer for subsequent analysis with Clampfit 8.1 software. Cell capacitance ranged between 14 and 18 pF and was measured with the cancellation circuitry in the voltage-clamp amplifier. Cells that displayed a noticeable shift in capacitance (> 0.3 pF) during experiments were excluded from analysis. A 1 M NaCl–agar salt bridge between the reference electrode and the bath solution was used to minimize offset potentials (< 2 mV). All experiments were performed at room temperature (20–22°C).

### Real-time PCR analysis of K<sub>IR</sub> subtypes

Smooth muscle cells (~200) isolated from middle cerebral, coronary septal and third-order mesenteric arteries were placed in RNase- and DNase-free collection tubes. Total RNA was extracted (RNeasy mini kit with DNAase treatment; Qiagen, Valencia, CA, USA) and first-strand cDNA synthesized using the Sensi-script RT kit (Qiagen) with oligo d(T) primer. To optimize reaction specificity, real-time PCR was initially performed with each primer set using rat brain cDNA, SYBR green (Bio-Rad, Hercules, CA, USA), and a range of annealing temperatures (52–62°C). Following melt-curve analysis,

1  $\mu$ l each reaction product was placed on a DNA 500 LabChip and examined using a bioanalyser (Model 2100, Agilent Technologies). A second aliquot of product was electrophoresed on a 1.5% (wt/vol) agarose gel, extracted using a gel extraction kit (Qiagen), and sequenced at the University of Calgary Core DNA facility. Having determined an ideal annealing temperature, real-time PCR efficiency was determined for all primer sets, with serial dilutions of brain cDNA used as template. Reaction efficiencies were as follows: KIR2.1, 94.4%; KIR2.2, 94.9%; KIR2.3, 98.8%; KIR2.4, 98.0%; and  $\beta$ -actin, 90.1%. The optimal real-time PCR reaction consisted of a hot start (95°C for 3 min) followed by 40 cycles of 95°C for 15 s, 55.1°C for 30 s and 72°C for 30 s. Samples were then exposed to a final extension period at 72°C for 10 min. A melt curve analysis was performed on each reaction and the threshold cycle determined using software provided with the Bio-Rad iCycler. K<sub>IR</sub> mRNA levels were standardized to  $\beta$ -actin. Forward (F) and reverse (R) primers were as follows: KIR2.1 (accession no. NM\_017296) (F) 5'-AGAGGAAGAGGACAGTGAGAAC-3', KIR2.1 (R) 5'-TCGCCTGGTTGTGGAGATC-3'; KIR2.2 (accession no. NM\_053981) (F) 5'-GCAGCCTTCTCTTCTCCA-TTGA-3', KIR2.2 (R) 5'-GACTGAGCCACCACCATGAAG-3'; KIR2.3 (accession no. NM\_053870) (F) 5'-CCTG-GACCGCATCTTCTTGG-3', KIR2.3 (R) 5'-CAGGAT-GACCACAATCTCAAAGTC-3'; KIR2.4 (accession no. NM\_170718) (F) 5'-ATGAGGTTGACTATCGACTT-CC-3', KIR2.4 (R) 5'-GGGAGCCAGGAAAACCTTGAC-TTA-3';  $\beta$ -actin (accession no. NM\_031144) (F) 5'-TATGAGGGTTACGCGCTCCC3' (R) 5'-ACGCTC-GGTCAGGATCTTCA3'. All smooth muscle cell samples were screened for template and endothelial cell contamination as previously described (Wu *et al.* 2007).

### Computational modelling

To strengthen our experimental approach, a computational model developed by Diep *et al.* (2005) predicted whether a smooth muscle K<sub>IR</sub>-like current could facilitate arterial hyperpolarization. Computational theory and base parameters were similar to those of the original model (Diep *et al.* 2005) with two notable exceptions. First, three additional layers of smooth muscle cells were added to our virtual artery, which is consistent with ultrastructural findings (Fig. 10). Second, the non-linear resistor representing the smooth muscle ionic conductance was divided into two components, one for K<sub>IR</sub> and the second for all other conductances. Based on the results of previous studies, we assumed that K<sub>IR</sub> was minimally active at –40 mV (0 pA), maximally active at –60 mV (2.0 pA) and reversed at –80 mV (Wu *et al.* 2007). A sigmoidal and exponential function fixed the data points between –40 and –60 mV, and –60 and –80 mV, respectively. At 2.0 pA, peak outward current would

be close to or below the resolution limit of whole-cell patch-clamp electrophysiology. The non-linear resistor representing all other smooth muscle conductances was comparable to that of Diep *et al.* (2005) except that its relative magnitude (below  $-40$  mV) was increased by 15%. Hyperpolarization was initiated by injecting 4.6 pA current into each smooth muscle cell for 500 ms. Voltage responses were subsequently monitored along the length of the virtual artery (2000  $\mu\text{m}$ ).

### Electron microscopy

Electron microscopy was conducted according to standard procedures (Sandow *et al.* 2002, 2004). In brief, anaesthetized rats were perfused via the left ventricle with saline (0.9% NaCl) containing 0.1% NaNO<sub>3</sub>, 0.1% bovine serum albumin and 5 U ml<sup>-1</sup> heparin at 25°C. Once cleared of blood, animals were fixed (10 min, 25°C) in 3% glutaraldehyde and 1% paraformaldehyde in 0.1 mM sodium cacodylate buffer with 0.2 mM CaCl<sub>2</sub>, 15 mM sucrose and 10 mM betaine (pH 7.35). Resistance arteries were then: (1) dissected free of surrounding tissue; (2) postfixed in a 2% osmium tetroxide buffer (2 h); (3) stained with saturated uranyl acetate (2 h); and (4) embedded in Araldite 502 according to conventional procedures (Sandow *et al.* 2002, 2004). Arteries were transversally sectioned (100 nm thick) and prepared for transmission electron microscopy (TEM). Selected areas were viewed on a Hitachi 7100 TEM and photographed on plate film.

### Chemicals, drugs and enzymes

Acetylcholine, BaCl<sub>2</sub>, bradykinin, buffer reagents, collagenases (types F and H), indomethacin,

N<sup>ω</sup>-nitro-L-arginine methyl ester (L-NAME), ouabain, phenylephrine, pinacidil and UTP were purchased from Sigma-Aldrich. Papain and P-1075 were acquired from Worthington (Lakewood, NJ, USA) and TOCRIS (Northfield, UK), respectively. When required, agents were dissolved in DMSO (final solvent concentration did not exceed 0.05%). All electron microscopy reagents were obtained from Electron Microscopy Sciences (Hatfield, PA, USA).

### Statistical analysis

Data are expressed as means  $\pm$  s.e.m. and *n* indicates the number of vessels or cells. No more than two experiments were performed on vessels or cells from a given animal. Paired *t* tests were performed to compare the effects of a given condition/treatment on arterial diameter,  $V_M$  or whole-cell current. *P* = 0.05 was considered statistically significant.

## Results

### K<sub>IR</sub> expression in vascular smooth muscle

In this study we characterized the diversity of smooth muscle K<sub>IR</sub> channel properties in middle cerebral, coronary septal and third-order mesenteric arteries. We began by monitoring the ability of precontracted resistance arteries, stripped of endothelium, to respond to elevated extracellular [K<sup>+</sup>] (from 5.8 to 15.8 mM), which augments K<sub>IR</sub> channel activity. Arteries were precontracted with elevated intravascular pressure and superfusion of phenylephrine in order to induce a depolarization that minimizes K<sub>IR</sub> activity under basal conditions. Elevated [K<sup>+</sup>] elicited a sustained Ba<sup>2+</sup>-sensitive dilatation in cerebral and coronary arteries (Fig. 1). No similar response

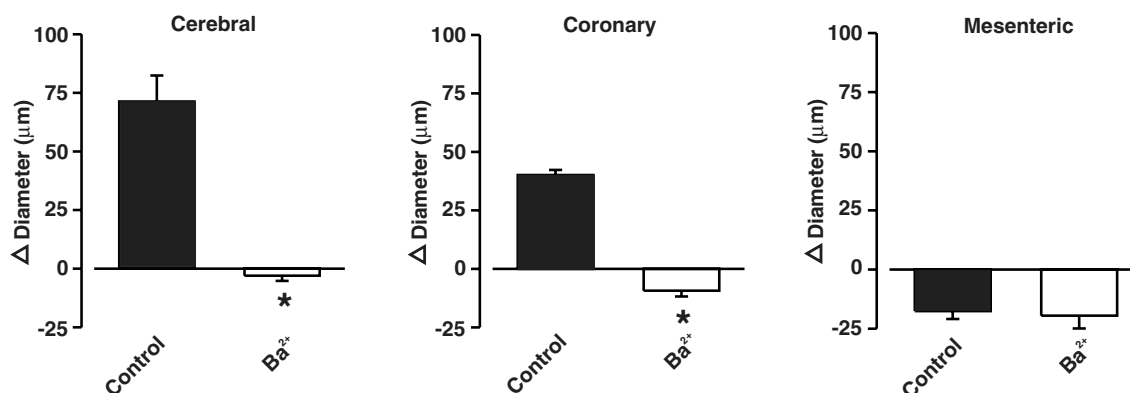


**Figure 1. K<sub>IR</sub> channels in cerebral and coronary arteries**

Middle cerebral (*n* = 6), coronary septal (*n* = 5) and third-order mesenteric (*n* = 6) arteries were cannulated and precontracted with elevated intravascular pressure (80 mmHg) and superfusion of phenylephrine (0.01–1  $\mu\text{M}$ ). Extracellular [K<sup>+</sup>] was elevated from 5.8 to 15.8 mM for 5 min and the sustained vasomotor response was monitored in the absence and presence of Ba<sup>2+</sup> (30  $\mu\text{M}$ ). Arterial diameter under control conditions, in the presence of Ba<sup>2+</sup> and in Ca<sup>2+</sup>-free media were as follows (in  $\mu\text{m}$ ): cerebral, 120  $\pm$  9, 115  $\pm$  11, 281  $\pm$  12; coronary, 123  $\pm$  15, 117  $\pm$  14, 199  $\pm$  11; mesenteric, 134  $\pm$  7, 127  $\pm$  12, 278  $\pm$  19.8, respectively. \*Significantly different from the control response.

was present in mesenteric arteries, which is suggestive of differential K<sub>IR</sub> expression. To better ascertain the variability in smooth muscle K<sub>IR</sub> expression, a range of molecular and electrophysiological approaches were subsequently employed. We first quantified the relative mRNA expression of K<sub>IR</sub>2.x subunits in smooth muscle cells isolated from the three vessel types. Figure 2 shows that K<sub>IR</sub>2.1 and 2.2 mRNA were present in all smooth muscle aliquots although the relative expression was ~2- to 6-fold higher in samples from cerebral and coronary arteries compared to mesenteric vessels. mRNA for K<sub>IR</sub>2.3 and 2.4 was absent from all smooth muscle aliquots. Western blot analysis confirmed the presence of K<sub>IR</sub>2.1/2.2 protein in whole arteries (data not shown). We did not, however, use this approach for cell-specific quantification because whole arteries contain several cell types that express K<sub>IR</sub> subunits. We also avoided immunocytochemistry given its limited quantitative power. Instead, patch-clamp electrophysiology was used to monitor the magnitude of the Ba<sup>2+</sup>-sensitive inward current. Figure 3 reveals that a Ba<sup>2+</sup>-sensitive inward current was prominent in smooth muscle cells from cerebral and coronary arteries. No similar current was present in mesenteric smooth muscle cells, which is consistent with low K<sub>IR</sub> expression. Despite this absence, inward current was sizable in mesenteric smooth muscle cells. The ionic basis of this current(s) remains unclear and warrants future investigation.

It is important to note that whereas K<sub>IR</sub> expression is low in mesenteric arteries, these arteries can dilate in response to elevated extracellular [K<sup>+</sup>] if the protocol is designed to stimulate the Na<sup>+</sup>-K<sup>+</sup> pump. For example, if resting extracellular [K<sup>+</sup>] was first reduced from 5.8 to 4 mM to decrease basal Na<sup>+</sup>-K<sup>+</sup>-ATPase activity, the subsequent elevation of extracellular [K<sup>+</sup>] did elicit a transient dilatation (Fig. 4A). This response often

displayed dilatation and was absent after the application of ouabain but not Ba<sup>2+</sup> (Fig. 4B and C).

### Defining negative slope conductance

With negative slope conductance proposed to be an important K<sub>IR</sub> property, we focused on documenting this biophysical characteristic. Vascular smooth muscle cells were enzymatically isolated and whole-cell patch-clamp electrophysiology used to quantify the outward component of the K<sub>IR</sub> current. Using bath and pipette solutions that facilitate current flow, a Ba<sup>2+</sup>-subtracted outward current, greater than 1.5 pA, was observed in smooth muscle cells isolated from cerebral (4 of 8; peak outward current, 4.7 ± 0.8 pA at -24.8 ± 2.6 mV) and coronary (3 of 6; peak outward current, 1.9 ± 0.7 pA at -15.0 ± 1.8 mV) arteries (Fig. 5). Although small in magnitude, negative slope conductance was readily observed between -10 and +10 mV. By contrast, outward current was not discernable in mesenteric smooth muscle cells (0 of 6). If negative slope conductance is important in arterial V<sub>M</sub> regulation, then micromolar levels of Ba<sup>2+</sup> should strongly depolarize arteries maintained at more negative potentials. Consistent with this prediction, the results in Fig. 6 illustrate that cerebral and coronary arteries stripped of endothelium and sustained in a hyperpolarized state (by lowering intravascular pressure) depolarized in response to superfused Ba<sup>2+</sup> (cerebral, 52.4 ± 1.2 to -36.2 ± 1.0 mV; coronary, -50.6 ± 1.4 to -35.2 ± 1.0 mV). When depolarized by high intravascular pressure and superfused phenylephrine, Ba<sup>2+</sup>-induced responses were reduced to < 2 mV (cerebral, -36.4 ± 2.1 to -35.4 ± 2.0 mV; coronary, -35.0 ± 0.5 to -34.1 ± 0.5 mV). Ba<sup>2+</sup>-induced depolarization was negligible in mesenteric arteries stripped of endothelium and maintained in a

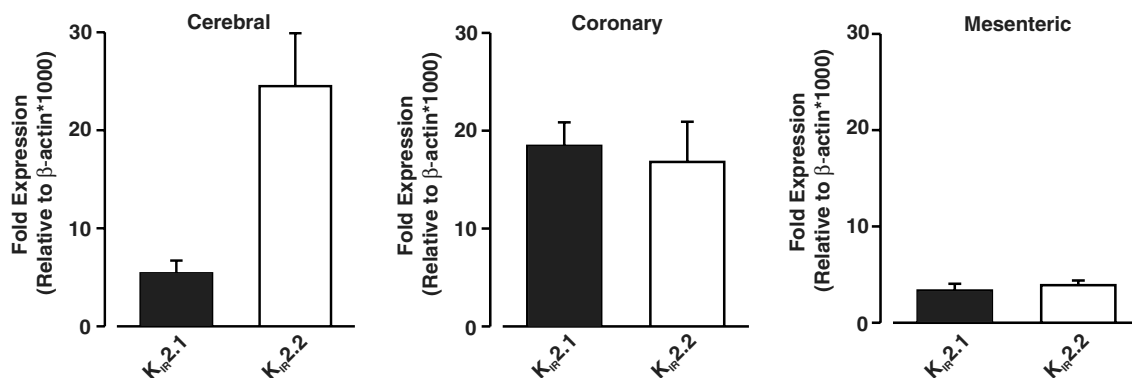


**Figure 2. Real-time PCR analysis of K<sub>IR</sub>2 subtypes**

mRNA expression of K<sub>IR</sub>2.1 and K<sub>IR</sub>2.2 in smooth muscle cells (~200) enzymatically isolated from middle cerebral (*n* = 8), coronary septal (*n* = 7) and third-order mesenteric (*n* = 8) arteries. Data are expressed relative to β-actin × 1000. Note that K<sub>IR</sub>2.3 and K<sub>IR</sub>2.4 mRNA was not detected in smooth muscle samples free of endothelial contamination.

hyperpolarized state by low intravascular pressure ( $-57.2 \pm 0.9$  to  $-55.8 \pm 1.1$  mV).

### Exploring electrical amplification

With knowledge of  $K_{IR}$  expression and negative slope conductance, next we investigated whether these channels amplify responses initiated by other  $K^+$  conductances. We began at a theoretical level with a computational model designed to mimic a multilayered artery. Under control conditions, the injection of 4.6 pA hyperpolarizing current into each smooth muscle cell reduced  $V_M$  from  $-40$  mV to approximately  $-55$  mV (Fig. 7). Consistent with the amplification concept, the removal of  $K_{IR}$  from the smooth muscle ionic representation attenuated hyperpolarization. To support these theoretical results, we examined whether  $Ba^{2+}$  application altered the ability of middle cerebral, coronary septal and third-order mesenteric arteries to respond to  $K^+$  channel activators. The results in Fig. 8 illustrate that  $30 \mu M$   $Ba^{2+}$  does attenuate  $K_{ATP}$ -induced dilatation in arteries that were de-endothelialized and which express smooth muscle  $K_{IR}$  channels (i.e. cerebral and coronary). By contrast,  $Ba^{2+}$  had little effect on  $K_{ATP}$ -induced responses in mesenteric

arteries where smooth muscle  $K_{IR}$  expression is limited. This unique pattern of  $Ba^{2+}$  attenuation extended to other agents including those that modulate endothelial  $K^+$  channels. This was evident in the experiments of Fig. 9 with endothelial-intact vessels, where superfused  $Ba^{2+}$  limited the ability of cerebral and coronary, but not mesenteric arteries to dilate in response to intraluminal UTP or superfused acetylcholine. These agents are known to activate endothelial  $Ca^{2+}$ -activated  $K^+$  channels (Marrelli *et al.* 2003; Crane *et al.* 2003a; Gluais *et al.* 2005; McNeish *et al.* 2006). Note that intraluminal UTP was employed in the cerebrovascular experiments because superfused acetylcholine did not elicit a significant endothelium-dependent response. The preceding experiments were conducted in the presence of L-NAME ( $50 \mu M$ ) and indomethacin ( $10 \mu M$ ) to limit nitric oxide and prostaglandin production, respectively. The inherent ability of the endothelium to hyperpolarize the overlying smooth muscle could arise from the expression of myo-endothelial gap junctions and the passage of charge between the two cell layers. As shown in Fig. 10, myo-endothelial contact sites were prevalent in all three vessel types. These structures formed at the tip of endothelial projections which penetrated through the

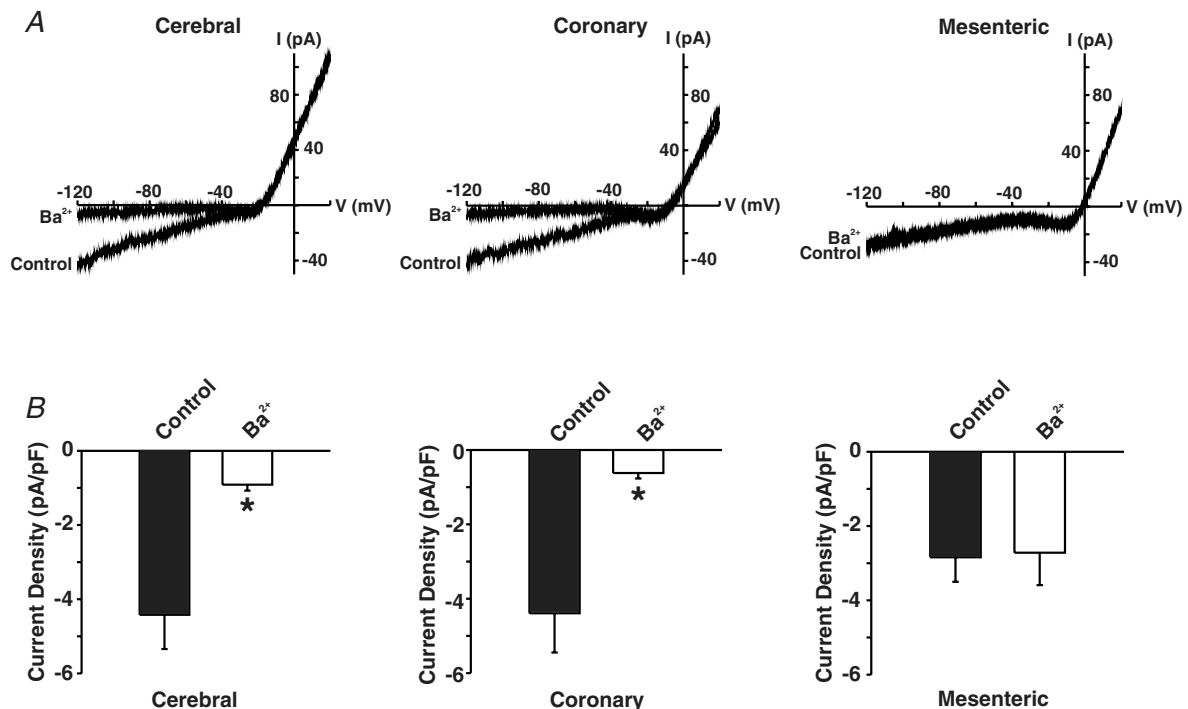


**Figure 3. The  $Ba^{2+}$ -sensitive  $K_{IR}$  current in vascular smooth muscle cells**

Whole-cell currents were monitored in middle cerebral, coronary septal and third-order mesenteric smooth muscle cells in the absence and presence of  $Ba^{2+}$  ( $30 \mu M$ ). The intra- and extracellular  $[K^+]$  were 120 and 60 mM, respectively. *A*, representative whole-cell current in the absence and presence of  $Ba^{2+}$ . *B*, peak inward current (at  $-120$  mV) in cerebral ( $n = 8$ ), coronary ( $n = 6$ ) and mesenteric ( $n = 6$ ) smooth muscle cells prior to and following  $Ba^{2+}$  application. \*Significantly different from control.

internal elastic lamina. High-resolution electron microscopy demonstrated gap junctional plaques at these sites of myo-endothelial contact.

## Discussion

In this study we examined whether smooth muscle K<sub>IR</sub> channels amplify arterial responses initiated by smooth muscle or endothelial K<sup>+</sup> conductances. To accomplish this objective it was necessary to: (1) characterize K<sub>IR</sub> expression in selected resistance arteries; (2) demonstrate negative slope conductance; and (3) determine whether K<sub>IR</sub> inhibition attenuates vessel responsiveness. Using a range of functional, molecular and electrophysiological approaches, initial observations revealed that smooth muscle K<sub>IR</sub> channels are highly expressed in middle cerebral and septal coronary but not third-order mesenteric arteries. When present, smooth muscle K<sub>IR</sub> channels were composed of K<sub>IR</sub>2.1 and 2.2 subunits and displayed negative slope conductance, which

is a key biophysical property that ensures that channel activity increases with hyperpolarization. Computational simulations subsequently revealed that negative slope conductance could amplify the hyperpolarization initiated by another vascular K<sup>+</sup> conductance. This prediction was verified experimentally in cerebral and coronary arteries where 30  $\mu$ M Ba<sup>2+</sup>, a K<sub>IR</sub> inhibitor, attenuated the ability of these vessels to dilate in response to smooth muscle and endothelial K<sup>+</sup> channel activators. Ba<sup>2+</sup>-induced attenuation was absent in mesenteric arteries, which are vessels with low K<sub>IR</sub> expression. Cumulatively, our findings demonstrate that when smooth muscle K<sub>IR</sub> channels are expressed, this conductance can function as an electrical amplifier.

## K<sub>IR</sub> expression in vascular smooth muscle

K<sub>IR</sub> channels are aptly named for their distinctive ability to pass current more readily in the inward direction. Structurally, these channels consist of four  $\alpha$ -subunits,

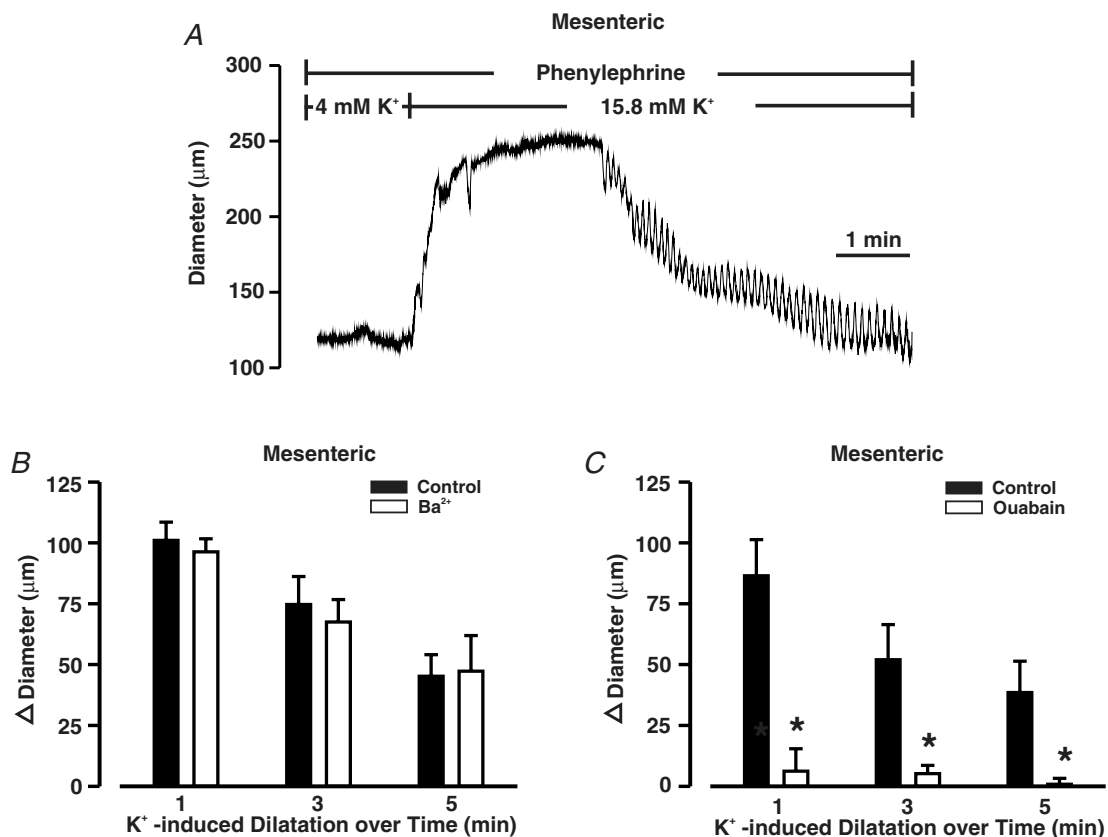


**Figure 4. Na<sup>+</sup>-K<sup>+</sup>-ATPase activation initiates transient dilatation in mesenteric arteries**

Third-order mesenteric arteries were cannulated and precontracted with elevated intravascular pressure (80 mmHg) and superfusion of phenylephrine (~1  $\mu$ M). Following equilibration, extracellular [K<sup>+</sup>] was reduced from 5.8 to 4.0 mM to decrease Na<sup>+</sup>-K<sup>+</sup>-ATPase activity. Extracellular [K<sup>+</sup>] was subsequently elevated to 15.8 mM eliciting a transient dilatation (A). This response was monitored in the absence and presence of Ba<sup>2+</sup> (A; 30  $\mu$ M; *n* = 6) or ouabain (B; 100 nM; *n* = 6). Arterial diameter in 4 mM K<sup>+</sup>, 4 mM K<sup>+</sup> + Ba<sup>2+</sup> or ouabain and in Ca<sup>2+</sup>-free media were (in  $\mu$ m): Fig. 5A; 121  $\pm$  8, 109  $\pm$  7, 277  $\pm$  17; Fig. 5B; 111  $\pm$  13, 89  $\pm$  13, 259  $\pm$  16. \*Significantly different from the control response.

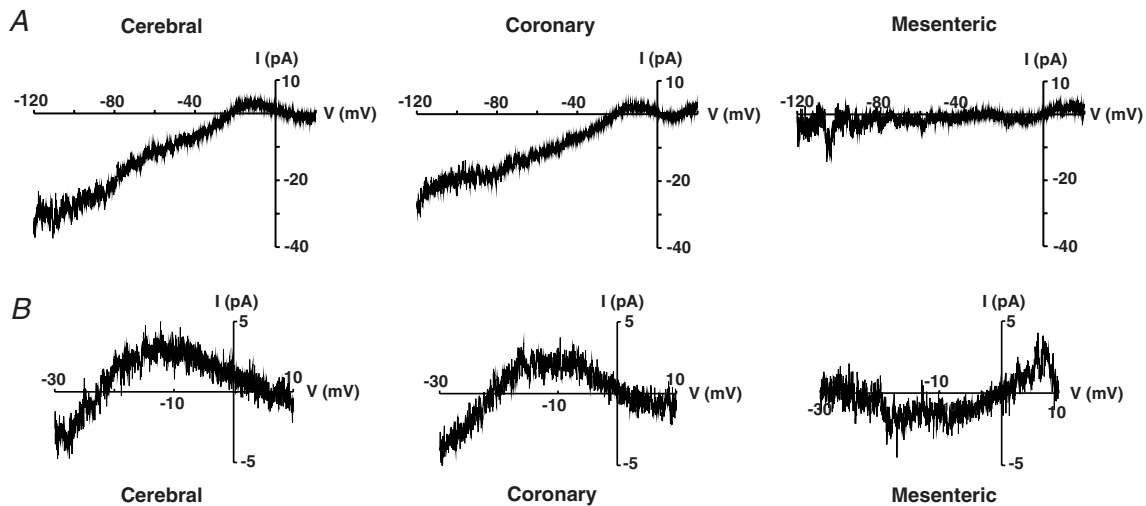


**Figure 5. Outward current through smooth muscle  $K_{IR}$  channels**

Whole-cell currents were monitored in middle cerebral, coronary septal and third-order mesenteric smooth muscle cells in the absence and presence of  $Ba^{2+}$  ( $30 \mu M$ ). The intra- and extracellular  $[K^+]$  were 120 and 60 mM, respectively. The outward component in A was magnified and replotted in B. Note that a small outward current, greater than 2 pA and with negative slope conductance was detectable in cerebral (4 of 8) and coronary (3 of 6) smooth muscle cells. No similar current was observed in mesenteric smooth muscle cells (0 of 6).

each composed of two transmembrane domains and a GYG-containing 'P loop' that confers selective  $K^+$  permeability (Quayle *et al.* 1997; Bichet *et al.* 2003). Molecular approaches have identified seven  $K_{IR}$  subfamilies, with  $K_{IR} 2.x$  channels readily expressed in excitable cells (Liu *et al.* 2001; Dhamoon *et al.* 2004; Wu *et al.* 2007). This subfamily is composed of four members with  $KIR2.1$  and  $2.2$  being present in vascular smooth muscle (Bradley *et al.* 1999; Karkanis *et al.* 2003; Wu *et al.* 2007). Although it is clear that smooth muscle  $K_{IR}$  channels are present in cerebral and coronary arteries (Quayle *et al.* 1993, 1996; Robertson *et al.* 1996), expression may not be

universal to all vascular beds (Crane *et al.* 2003b). Indeed, past studies have implied, from limited observations, that smooth muscle  $K_{IR}$  channels are poorly expressed in the mesenteric circulation (Crane *et al.* 2003b; Brochet & Langton, 2006). To better understand channel expression patterns, we characterized the properties of smooth muscle  $K_{IR}$  channels in middle cerebral, coronary septal and third-order mesenteric arteries. This characterization began at a functional level where elevated extracellular  $[K^+]$  (5.8–15.8 mM) was used to augment  $K_{IR}$  activity and dilate resistance arteries precontracted with elevated intravascular pressure and superfusion of phenylephrine.

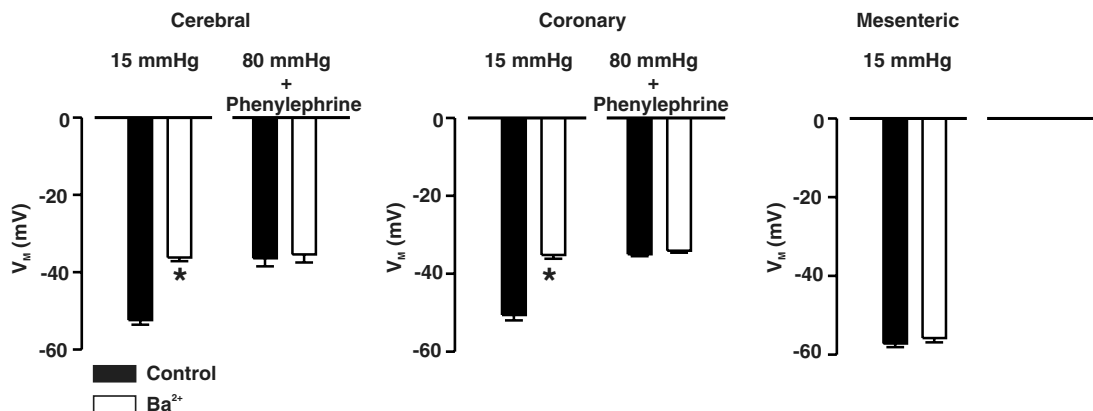


**Figure 6. The effects of  $Ba^{2+}$  on arterial membrane potential ( $V_M$ )**

Middle cerebral ( $n = 5$ ), coronary septal ( $n = 6$ ) and third-order mesenteric ( $n = 5$ ) arteries were cannulated and maintained in either a hyperpolarized (intravascular pressure, 15 mmHg) or depolarized (intravascular pressure, 80 mmHg; superfused phenylephrine,  $0.01\text{--}1 \mu M$ ) state. Arterial  $V_M$  was monitored in the absence and presence of  $Ba^{2+}$  ( $30 \mu M$ ). \*Significantly different from control  $V_M$ .

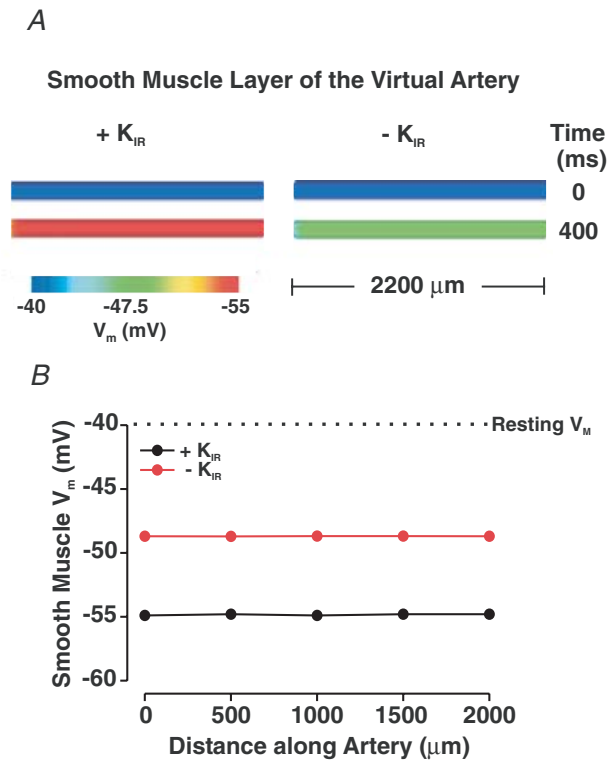


**Figure 7. Computational modelling predicts that K<sub>IR</sub> channels amplify hyperpolarization**

Simulation: a hyperpolarizing current was injected (4.6 pA for 500 ms) into each smooth muscle cell of a virtual artery composed of one endothelial layer and four smooth muscle layers. Membrane potential responses were monitored (at 500 ms) in the outer smooth muscle cell layer in the presence and absence of a smooth muscle K<sub>IR</sub>-like current. These responses were colour-mapped along the vessel wall (A) or were presented in a two-dimensional voltage plot (B).

As is evident in Fig. 1, this perturbation elicited a differential response with cerebral and coronary arteries dilating in a Ba<sup>2+</sup>-sensitive manner, but with mesenteric vessels failing to respond similarly. With these functional

observations implying variable K<sub>IR</sub> expression, we subsequently isolated smooth muscle cells and utilized real-time PCR to quantify mRNA expression. This analysis revealed that whereas KIR2.1/2.2 mRNA was present in all vascular beds, expression levels were 2- to 6-fold higher in smooth muscle cells from cerebral and coronary arteries than those from the mesenteric circulation (Fig. 2). Whereas Western blot analysis verified K<sub>IR</sub> protein expression (data not shown), the mixed nature of a whole vessel renders this approach inappropriate to quantify differential channel expression. Immunocytochemistry was also avoided due its limited quantitative power. Instead, the magnitude of the Ba<sup>2+</sup>-sensitive inward current was examined in smooth muscle cells isolated from the three vascular beds. Consistent with our functional and molecular observations, a Ba<sup>2+</sup>-sensitive inward current was detected in smooth muscle cells from cerebral and coronary arteries (Fig. 3). The magnitude of this current was comparable to that previously observed (Quayle *et al.* 1993, 1996; Robertson *et al.* 1996) and was not present in mesenteric smooth muscle cells. Overall, this work is the first to illustrate a consistent pattern of greater smooth muscle K<sub>IR</sub> expression in cerebral and coronary arteries than in the mesenteric circulation.

Although K<sub>IR</sub> expression is low in mesenteric smooth muscle cells, it should be stated that this absence does not preclude these vessels from dilating in response to certain K<sup>+</sup> challenges. Indeed, as highlighted in Fig. 4, mesenteric arteries can dilate in response to 15.8 mM K<sup>+</sup> if resting extracellular [K<sup>+</sup>] is reduced to 4.0 mM prior to stimulation. This reduction in resting extracellular [K<sup>+</sup>] presumably enables mesenteric dilatation via limited basal Na<sup>+</sup>-K<sup>+</sup>-ATPase activity, thereby making the pump available for subsequent stimulation (Brochet & Langton, 2006). This view is consistent with the transient nature of the dilatatory response along with its documented ouabain sensitivity (Fig. 4).

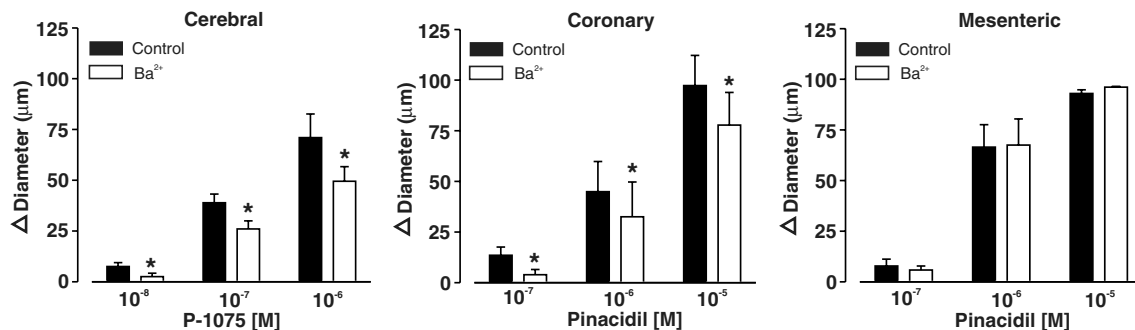


**Figure 8. The effects of Ba<sup>2+</sup> on K<sub>ATP</sub>-induced vasodilatation**

Middle cerebral (*n* = 6), coronary septal (*n* = 6) and third-order mesenteric (*n* = 6) arteries were cannulated and precontracted with elevated intravascular pressure (80 mmHg) and superfusion of phenylephrine (0.01–1 μM). Vasodilatory responses to K<sub>ATP</sub> openers (P-1075 or pinacidil) were monitored in the absence or presence of Ba<sup>2+</sup> (30 μM). Arterial diameter under control conditions, in the presence of Ba<sup>2+</sup> and in Ca<sup>2+</sup>-free media were as follows (in μm): cerebral, 125 ± 7, 115 ± 8, 249 ± 7; coronary, 137 ± 21, 135 ± 16, 262 ± 29; mesenteric, 77 ± 5, 76 ± 5, 256 ± 18, respectively. \*Significantly different control K<sub>ATP</sub>-induced dilatation.

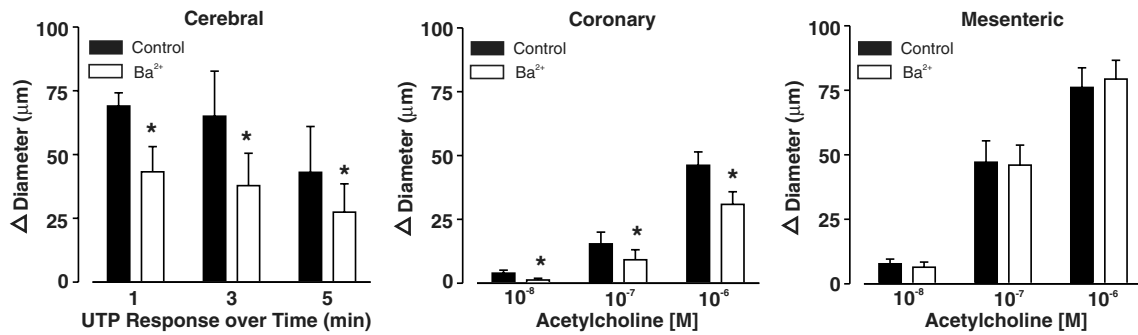


**Figure 9. Effects of Ba<sup>2+</sup> on endothelium-induced vasodilatation**

Middle cerebral ( $n = 6$ ), coronary septal ( $n = 6$ ) and third-order mesenteric ( $n = 6$ ) arteries were cannulated and precontracted with elevated intravascular pressure (80 mmHg) and superfusion of phenylephrine (0.01–1  $\mu\text{M}$ ). L-NAME (100  $\mu\text{M}$ ) and indomethacin (10  $\mu\text{M}$ ) were added to attenuate nitric oxide and prostaglandin production, respectively. Dilatory responses to intraluminal UTP (cerebral) or superfused acetylcholine (coronary and mesenteric) were monitored in the absence or presence of Ba<sup>2+</sup> (30  $\mu\text{M}$ ). Arterial diameter under control conditions, in the presence of Ba<sup>2+</sup> and in Ca<sup>2+</sup>-free media were as follows (in  $\mu\text{m}$ ): cerebral, 214  $\pm$  10, 204  $\pm$  9, 302  $\pm$  8; coronary, 146  $\pm$  17, 135  $\pm$  14, 269  $\pm$  17; mesenteric 89  $\pm$  7, 87  $\pm$  5, 247  $\pm$  19, respectively. \*Significantly different control dilatation.

### Defining negative slope conductance

Although strong inward rectification is one of the defining characteristics of smooth muscle K<sub>IR</sub> channels, it is the

small outward component with its intrinsic property of negative slope conductance which may be important for the regulation of arterial tone. As such, in this study we focused on documenting this biophysical property. In the

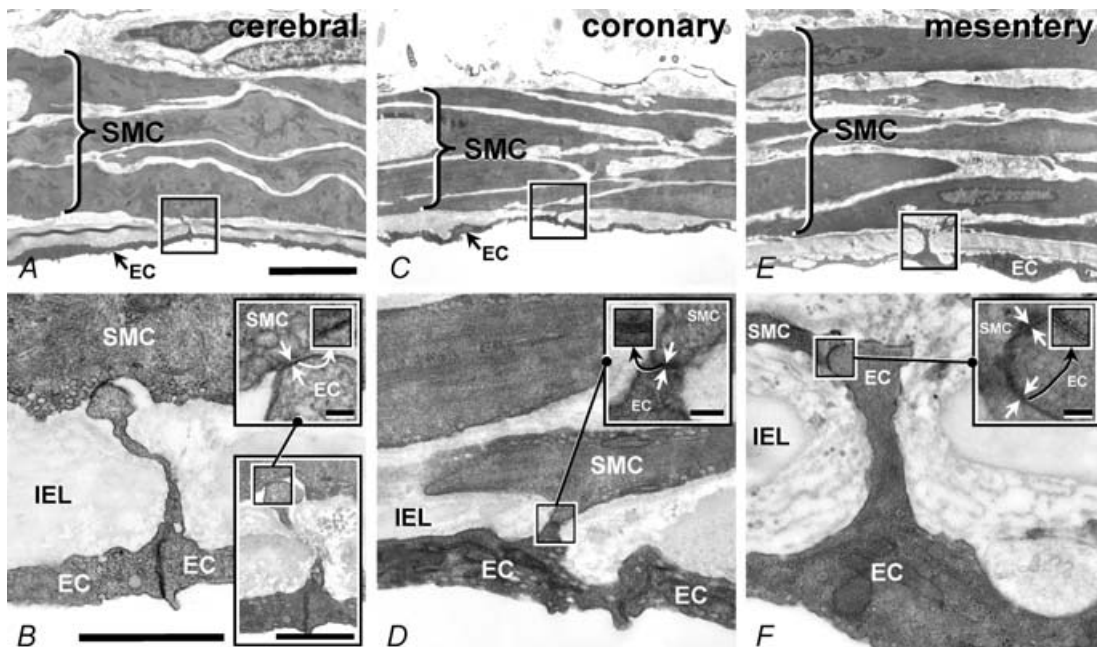


**Figure 10. Myo-endothelial gap junctions in the arterial wall**

Middle cerebral (A and D) coronary septal (B and E) and third-order mesenteric (C and F) arteries were isolated and prepared for electron microscopy. Myo-endothelial gap junctions with their characteristic pentalaminar appearance were common in these vessels; gap junctional plaques between endothelial cells were also evident (B and D; between arrowheads). Area within square in A, C and E corresponds to the main panels in B, D and F, respectively. Insets in B, D and F are shown in upper right of each respective panel. In B (main), the endothelial 'stalk' makes contact with an adjacent smooth muscle cell, while two serial sections later (lower inset), the myo-endothelial contact site reveals its typical pentalaminar appearance (upper inset). Middle cerebral, coronary septal and third-order mesenteric arteries had 3.8  $\pm$  0.2, 4.2  $\pm$  0.2 and 4.8  $\pm$  0.2 smooth muscle cell layers, respectively ( $n = 3$ ). Scale bar: A, C and E, 5  $\mu\text{m}$ ; B, D and F (and B, lower inset), 1  $\mu\text{m}$ ; B, D and F (upper inset), 50 nm.

past, such documentation has proven difficult because outward current is limited and close to the resolution limits of a patch-clamp amplifier (Quayle *et al.* 1993, 1996; Robertson *et al.* 1996; Wu *et al.* 2007). However, by carefully designing the bath and pipette solutions to augment  $K_{IR}$  activity, an outward current, greater than 2 pA and with negative slope conductance was resolvable in 50% of the smooth muscle cells from cerebral and coronary arteries (Fig. 5). Peak outward current did not exceed 5 pA and, as expected, a similar current was not apparent in mesenteric smooth muscle cells. Although the preceding single-cell results are important, they alone do not demonstrate that this biophysical property is present in intact arteries. To address this concern, we measured arterial  $V_M$  and the effects of  $Ba^{2+}$  on vessels maintained at different resting potentials through manipulation of intravascular pressure and superfusion of phenylephrine. The logic underlying this approach centres on the idea that if negative slope conductance is present, then  $Ba^{2+}$  should have a greater electrical effect on arteries held at more negative potentials. Consistent with its functional occurrence, micromolar levels of  $Ba^{2+}$  strongly depolarized ( $\sim 15$  mV)  $K_{IR}$ -expressing arteries maintained in a hyperpolarized state by low intravascular pressure (Fig. 6). At more depolarized potentials where outward  $K_{IR}$  current should be limited,  $Ba^{2+}$ -induced depolarization was restricted to  $< 2$  mV. In mesenteric arteries where smooth muscle  $K_{IR}$  expression was low,  $Ba^{2+}$  application had little discernable effect on resting  $V_M$ . This latter experiment is an important control as it demonstrates that at  $30 \mu M$ ,  $Ba^{2+}$  does not substantively affect other channels involved in  $V_M$  regulation. This is an important consideration because at submillimolar concentrations, this divalent cation can attenuate the activity of  $K_{ATP}$  and twin-pore  $K^+$  channels (Nelson *et al.* 1990; Nelson & Quayle, 1995; Campanucci *et al.* 2003).

### Exploring electrical amplification

Lastly, with knowledge of vascular smooth muscle  $K_{IR}$  properties, we focused on whether these channels amplify responses initiated by other smooth muscle or endothelial  $K^+$  conductances. As stated previously, our interest in this channel stems from the intrinsic property of negative slope conductance. Briefly, negative slope conductance refers to the inherent ability of  $K_{IR}$  channels to increase their activity as a cell hyperpolarizes (Nelson *et al.* 1990; Nelson & Quayle, 1995). This rise depends on the relief of a voltage-dependent  $Mg^{2+}$ /polyamine block (Nelson & Quayle, 1995; Robertson *et al.* 1996; Matsuda *et al.* 2003). Our work began at a theoretical level with the use of a computational model to explore whether a smooth muscle  $K_{IR}$  current alters the ability of a multilayered artery to hyperpolarize (Fig. 7). The  $K_{IR}$  current employed in this model retained negative

slope conductance and was designed to be minimally and maximally active at  $-40$  and  $-60$  mV, respectively. Peak outward current was set to 2 pA, a value consistent with a limited set of observations gathered at physiological  $[K^+]$  (Wu *et al.* 2007). In keeping with the amplification concept, the hyperpolarization induced by smooth muscle current injection decreased in the absence of  $K_{IR}$  (Fig. 7). This attenuation approached 35% and a change of this magnitude should, under experimental conditions, impair arterial dilatation. To verify this prediction, we examined the ability of  $K_{IR}$  expressing (cerebral/coronary) and nominally expressing (mesenteric) arteries to dilate in response to  $K^+$  channel activators in the presence and absence of  $30 \mu M Ba^{2+}$ . In these experiments, all arteries were precontracted with elevated intravascular pressure and superfusion of phenylephrine, which will induce depolarization and minimize  $K_{IR}$  activity under basal conditions. Consistent with theoretical predictions, initial experiments with de-endothelialized vessels reveal that  $Ba^{2+}$  attenuated the ability of presumed  $K_{ATP}$  activators to dilate cerebral and coronary arteries (Fig. 8). This reduction occurred over a range of concentrations and was absent in mesenteric arteries, which show low  $K_{IR}$  expression. A similar pattern of attenuation was observed in a second experimental set where the endothelium was retained and intraluminal UTP or superfused acetylcholine was used to activate small- and/or intermediate-conductance  $Ca^{2+}$ -activated  $K^+$  channels (Fig. 9) (Marrelli *et al.* 2003; Crane *et al.* 2003a; Gluais *et al.* 2005; McNeish *et al.* 2006). It is interesting to note that L-NAME and indomethacin were included in the latter experiments. As such, it can be argued that the endothelium is driving the smooth muscle responses through a nitric oxide- and prostaglandin-independent event. The nature of this event is unclear but could involve the production of an arachidonic acid metabolite (Campbell *et al.* 1996; Bryan *et al.* 2006; Marrelli *et al.* 2007) or perhaps hydrogen peroxide (Hatoum *et al.* 2005). Alternatively, charge could directly spread from the endothelium to the overlying smooth muscle layers via myo-endothelial gap junctions (Emerson & Segal, 2000; Sandow *et al.* 2002; Sokoya *et al.* 2007). Previous studies have provided both direct and indirect evidence for these junctions in cerebral, coronary and mesenteric arteries (Edwards *et al.* 1998; Edwards *et al.* 2000; Mather *et al.* 2006). Consistent with these observations and the concept of direct charge transfer, high-resolution electron microscopy illustrated that myo-endothelial gap junctions were prevalent in all three arteries (Fig. 10). These junctions occur at the tip of endothelial cell projections which pass through the internal elastic lamina to make contact with the overlying smooth muscle.

As a final note, it is important to recognize that while this study is the first to associate negative slope conductance

with the facilitation of endothelium-dependent responses, it is not the first to implicate smooth muscle  $K_{IR}$  channels in such a process (Edwards *et al.* 1998; Edwards & Weston, 2004). Indeed, Edwards & Weston (2004) have previously drawn this connection, although unlike in this investigation, negative slope conductance was not considered. Rather, these authors proposed that  $K_{IR}$  channels were directly activated by the  $K^+$  release from endothelial cells (Edwards *et al.* 1998; Edwards & Weston, 2004). This is an interesting hypothesis although one that is difficult to resolve given that the relative area of the endothelium is small compared to the extracellular space. As such, it would be difficult to sustain a millimolar rise in extracellular  $[K^+]$  without inducing a substantial depletion of intracellular  $[K^+]$ . Such a depletion would elicit a rightward shift in the  $K^+$  equilibrium potential and in a counterproductive manner limit arterial hyperpolarization.

### Limitations

We acknowledge three important concerns in the manner in which the preceding observations are interpreted. First, we recognize that  $K_{IR}$  channels may be present in endothelial cells (Nilius & Droogmans, 2001; Fang *et al.* 2005), and thus part of the  $Ba^{2+}$ -induced attenuation observed in Fig. 9 could result from their inhibition. Second, we are aware that not all arteries need to express smooth muscle  $K_{IR}$  channels to elicit robust dilatory responses. This was evident from the mesenteric observations and it raises a series of intriguing biophysical questions for further investigation. Finally, we acknowledge that in addition to amplifying hyperpolarization, negative slope conductance could facilitate depolarization. Current experimental approaches do not, however, allow this possibility to be systematically tested.

### Summary

The results of this study demonstrate that smooth muscle  $K_{IR}$  channels, when present, play an important role in amplifying electrical and vasomotor responses initiated by vascular  $K^+$  channels. Amplification was ascribed to negative slope conductance, a biophysical property which enables  $KIR2.1/2.2$  activity to increase with hyperpolarization. Broadly speaking, our findings illustrate that subtle channel properties are important for the regulation of arterial responsiveness. They also show that when an agonist alters the electrical state of a multilayered artery, the ion channels underlying this response are not always under the direct regulatory control of the stimulus.

### References

- Bayliss WM (1902). On the local reactions of the arterial wall to changes in internal pressure. *J Physiol* **28**, 220–231.
- Bichet D, Haass FA & Jan LY (2003). Merging functional studies with structures of inward-rectifier  $K^+$  channels. *Nat Rev Neurosci* **4**, 957–967.
- Bradley KK, Jaggar JH, Bonev AD, Heppner TJ, Flynn ER, Nelson MT & Horowitz B (1999). Kir2.1 encodes the inward rectifier potassium channel in rat arterial smooth muscle cells. *J Physiol* **515**, 639–651.
- Brayden JE & Bevan JA (1985). Neurogenic muscarinic vasodilation in the cat. An example of endothelial cell-independent cholinergic relaxation. *Circ Res* **56**, 205–211.
- Brochet DX & Langton PD (2006). Dual effect of initial  $[K]$  on vascular tone in rat mesenteric arteries. *Pflugers Arch* **453**, 33–41.
- Bryan RM Jr, You J, Phillips SC, Andresen JJ, Lloyd EE, Rogers PA, Dryer SE & Marrelli SP (2006). Evidence for two-pore domain potassium channels in rat cerebral arteries. *Am J Physiol Heart Circ Physiol* **291**, H770–H780.
- Campanucci VA, Fearon IM & Nurse CA (2003). A novel  $O_2$ -sensing mechanism in rat glossopharyngeal neurones mediated by a halothane-inhibitable background  $K^+$  conductance. *J Physiol* **548**, 731–743.
- Campbell WB, Gebremedhin D, Pratt PF & Harder DR (1996). Identification of epoxyeicosatrienoic acids as endothelium-derived hyperpolarizing factors. *Circ Res* **78**, 415–423.
- Crane GJ, Gallagher N, Dora KA & Garland CJ (2003a). Small- and intermediate-conductance calcium-activated  $K^+$  channels provide different facets of endothelium-dependent hyperpolarization in rat mesenteric artery. *J Physiol* **553**, 183–189.
- Crane GJ, Walker SD, Dora KA & Garland CJ (2003b). Evidence for a differential cellular distribution of inward rectifier K channels in the rat isolated mesenteric artery. *J Vasc Res* **40**, 159–168.
- Dhamoon AS, Pandit SV, Sarmast F, Parisian KR, Guha P, Li Y, Bagwe S, Taffet SM & Anumonwo JM (2004). Unique Kir2.x properties determine regional and species differences in the cardiac inward rectifier  $K^+$  current. *Circ Res* **94**, 1332–1339.
- Diep HK, Vigmond EJ, Segal SS & Welsh DG (2005). Defining electrical communication in skeletal muscle resistance arteries: a computational approach. *J Physiol* **568**, 267–281.
- Edwards G, Dora KA, Gardener MJ, Garland CJ & Weston AH (1998).  $K^+$  is an endothelium-derived hyperpolarizing factor in rat arteries. *Nature* **396**, 269–272.
- Edwards G, Thollon C, Gardener MJ, Feletou M, Vilaine J, Vanhoutte PM & Weston AH (2000). Role of gap junctions and EETs in endothelium-dependent hyperpolarization of porcine coronary artery. *Br J Pharmacol* **129**, 1145–1154.
- Edwards G & Weston AH (2004). Potassium and potassium clouds in endothelium-dependent hyperpolarizations. *Pharmacol Res* **49**, 535–541.
- Emerson GG & Segal SS (2000). Electrical coupling between endothelial cells and smooth muscle cells in hamster feed arteries: role in vasomotor control. *Circ Res* **87**, 474–479.

- Fang Y, Schram G, Romanenko V, Shi C, Conti L, Vandenberg CA, Davies PF, Nattel S & Levitan I (2005). Functional expression of Kir2.x in human aortic endothelial cells: the dominant role of Kir2.2. *Am J Physiol Cell Physiol* **289**, C1134–C1144.
- Filosa JA, Bonev AD, Straub SV, Meredith AL, Wilkerson MK, Aldrich RW & Nelson MT (2006). Local potassium signaling couples neuronal activity to vasodilation in the brain. *Nat Neurosci* **9**, 1397–1403.
- Garcia-Roldan JL & Bevan JA (1990). Flow-induced constriction and dilation of cerebral resistance arteries. *Circ Res* **66**, 1445–1448.
- Gluais P, Edwards G, Weston AH, Falck JR, Vanhoutte PM & Feletou M (2005). Role of SK<sub>Ca</sub> and IK<sub>Ca</sub> in endothelium-dependent hyperpolarizations of the guinea-pig isolated carotid artery. *Br J Pharmacol* **144**, 477–485.
- Harder DR, Alkayed NJ, Lange AR, Gebremedhin D & Roman RJ (1998). Functional hyperemia in the brain: hypothesis for astrocyte-derived vasodilator metabolites. *Stroke* **29**, 229–234.
- Hatoum OA, Binion DG, Miura H, Telford G, Otterson MF & Gutterman DD (2005). Role of hydrogen peroxide in ACh-induced dilation of human submucosal intestinal microvessels. *Am J Physiol Heart Circ Physiol* **288**, H48–H54.
- Karkanis T, Li S, Pickering JG & Sims SM (2003). Plasticity of Kir channels in human smooth muscle cells from internal thoracic artery. *Am J Physiol Heart Circ Physiol* **284**, H2325–H2334.
- Knot HJ & Nelson MT (1998). Regulation of arterial diameter and wall [Ca<sup>2+</sup>] in cerebral arteries of rat by membrane potential and intravascular pressure. *J Physiol* **508**, 199–209.
- Koller A & Kaley G (1991). Endothelial regulation of wall shear stress and blood flow in skeletal muscle microcirculation. *Am J Physiol Heart Circ Physiol* **260**, H862–H868.
- Liu GX, Derst C, Schlichthorl G, Heinen S, Seebohm G, Bruggemann A, Kummer W, Veh RW, Daut J & Preisig-Muller R (2001). Comparison of cloned Kir2 channels with native inward rectifier K<sup>+</sup> channels from guinea-pig cardiomyocytes. *J Physiol* **532**, 115–126.
- Luykenaar KD, Brett SE, Wu BN, Wiehler WB & Welsh DG (2004). Pyrimidine nucleotides suppress K<sub>DR</sub> currents and depolarize rat cerebral arteries by activating Rho kinase. *Am J Physiol Heart Circ Physiol* **286**, H1088–H1100.
- McNeish AJ, Sandow SL, Neylon CB, Chen MX, Dora KA & Garland CJ (2006). Evidence for involvement of both IK<sub>Ca</sub> and SK<sub>Ca</sub> channels in hyperpolarizing responses of the rat middle cerebral artery. *Stroke* **37**, 1277–1282.
- Marrelli SP, Eckmann MS & Hunte MS (2003). Role of endothelial intermediate conductance K<sub>Ca</sub> channels in cerebral EDHF-mediated dilations. *Am J Physiol Heart Circ Physiol* **285**, H1590–H1599.
- Marrelli SP, O'Neil RG, Brown RC & Bryan RM Jr (2007). PLA2 and TRPV4 channels regulate endothelial calcium in cerebral arteries. *Am J Physiol Heart Circ Physiol* **292**, H1390–H1397.
- Mather S, Dora KA, Sandow SL, Winter P & Garland CJ (2006). Rapid endothelial cell-selective loading of connexin 40 antibody blocks endothelium-derived hyperpolarizing factor dilation in rat small mesenteric arteries. *Circ Res* **97**, 399–407.
- Matsuda H, Oishi K & Omori K (2003). Voltage-dependent gating and block by internal spermine of the murine inwardly rectifying K<sup>+</sup> channel, Kir2.1. *J Physiol* **548**, 361–371.
- Nelson MT, Patlak JB, Worley JF & Standen NB (1990). Calcium channels, potassium channels, and voltage dependence of arterial smooth muscle tone. *Am J Physiol Cell Physiol* **259**, C3–C18.
- Nelson MT & Quayle JM (1995). Physiological roles and properties of potassium channels in arterial smooth muscle. *Am J Physiol Cell Physiol* **268**, C799–C822.
- Nilius B & Droogmans G (2001). Ion channels and their functional role in vascular endothelium. *Physiol Rev* **81**, 1415–1459.
- Quayle JM, Dart C & Standen NB (1996). The properties and distribution of inward rectifier potassium currents in pig coronary arterial smooth muscle. *J Physiol* **494**, 715–726.
- Quayle JM, McCarron JG, Brayden JE & Nelson MT (1993). Inward rectifier K<sup>+</sup> currents in smooth muscle cells from rat resistance-sized cerebral arteries. *Am J Physiol Cell Physiol* **265**, C1363–C1370.
- Quayle JM, Nelson MT & Standen NB (1997). ATP-sensitive and inwardly rectifying potassium channels in smooth muscle. *Physiol Rev* **77**, 1165–1232.
- Robertson BE, Bonev AD & Nelson MT (1996). Inward rectifier K<sup>+</sup> currents in smooth muscle cells from rat coronary arteries: block by Mg<sup>2+</sup>, Ca<sup>2+</sup>, and Ba<sup>2+</sup>. *Am J Physiol Heart Circ Physiol* **271**, H696–H705.
- Sandow SL, Goto K, Rummery NM & Hill CE (2004). Developmental changes in myo-endothelial gap junction mediated vasodilator activity in the rat saphenous artery. *J Physiol* **556**, 875–876.
- Sandow SL, Tare M, Coleman HA, Hill CE & Parkington HC (2002). Involvement of myo-endothelial gap junctions in the actions of endothelium-derived hyperpolarizing factor. *Circ Res* **90**, 1108–1113.
- Schram G, Pourrier M, Wang Z, White M & Nattel S (2003). Barium block of Kir2 and human cardiac inward rectifier currents: evidence for subunit-heteromeric contribution to native currents. *Cardiovasc Res* **59**, 328–338.
- Segal SS (2000). Integration of blood flow control to skeletal muscle: key role of feed arteries. *Acta Physiol Scand* **168**, 511–518.
- Segal SS & Duling BR (1986). Communication between feed arteries and microvessels in hamster striated muscle: segmental vascular responses are functionally coordinated. *Circ Res* **59**, 283–290.
- Si ML & Lee TJ (2002).  $\alpha$ 7-nicotinic acetylcholine receptors on cerebral perivascular sympathetic nerves mediate choline-induced nitergic neurogenic vasodilation. *Circ Res* **91**, 62–69.
- Sokoya EM, Burns AR, Setiawan CT, Coleman HA, Parkington HC & Tare M (2007). Evidence for the involvement of myo-endothelial gap junctions in EDHF-mediated relaxation in the rat middle cerebral artery. *Am J Physiol Heart Circ Physiol* **291**, H385–H393.
- Somlyo AP & Somlyo AV (2003). Ca<sup>2+</sup> sensitivity of smooth muscle and nonmuscle myosin II: modulated by G proteins, kinases, and myosin phosphatase. *Physiol Rev* **83**, 1325–1358.

- Welsh DG & Brayden JE (2001). Mechanisms of coronary artery depolarization by uridine triphosphate. *Am J Physiol Heart Circ Physiol* **280**, H2545–H2553.
- Wu BN, Luykenaar KD, Brayden JE, Giles WR, Corteling RL, Wiehler WB & Welsh DG (2007). Hyposmotic challenge inhibits inward rectifying K<sup>+</sup> channels in cerebral arterial smooth muscle cells. *Am J Physiol Heart Circ Physiol* **292**, H1085–H1094.

### Acknowledgements

The authors would like to acknowledge the technical assistance of Hai Kim Diep, Jaya Tunuguntla and Xuansha Chen. This work was supported by an operating grant from the Canadian Institute for Health Research (D.W.) and National Health and Medical Research Council of Australia (ID 401112 and 455243 to S.L.S.). D.W. is a senior scholar with the Alberta Heritage Foundation for Medical Research and holds a Canada Research Chair.